Open Access

Enhancing Propagation Length of Surface Plasmon Polaritons by Using Metallic Double-Layer Structure
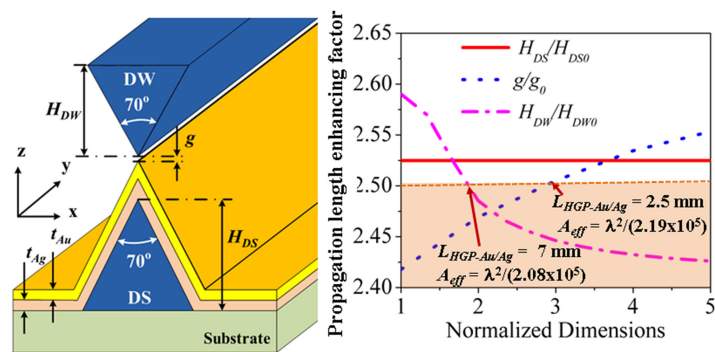
Manh Hoang Chu
Minh-Tuan Trinh

photonics
SOCIETY

IEEE

Enhancing Propagation Length of Surface Plasmon Polaritons by Using Metallic Double-Layer Structure

Manh Hoang Chu [ID] [1] **and Minh-Tuan Trinh**[2]

[1]International Training Institute for Materials Science, Hanoi University of Science and Technology, Hanoi 10000, Vietnam
[2]Department of Electrical Engineering and Computer Science, University of Michigan, Ann Arbor, MI 48109 USA

Abstract: In this paper, we propose to use a wedge-shaped plasmonic waveguide with a metallic double-layer structure for improving the propagation length of surface plasmon polaritons. The wedge silicon waveguide is covered by a first layer of Ag and by a second layer of Au outermost in which the former has a good lightwave guiding property but unstable to the operating medium and the latter is more stable to the operating medium. Numerically investigated results show that the propagation length of surface plasmon polaritons using the Au/Ag double-layer structure with an appropriate thickness of the Au covering layer can be increased by a factor of 2.5 compared to that of using the only Au metallic structure at the same propagation mode area. The advantage of the proposed metallic double-layer structure is also preserved in hybrid plasmonic waveguides.

Index Terms: Plasmonic waveguide, sub-wavelength light wave guiding, metallic double-layer structure.

1. Introduction

Recently, surface plasmon polariton (SPP) has attracted intensively research interest for various applications in nanophotonics such as nanolasers, optical switching, optical modulators, and plasmonic waveguides [1]–[7]. Among these functional devices, plasmonic waveguide is an attractive research area which can be found in various applications, such as light signal guiding and modulating far beyond the diffraction limit [5]–[12], ultracompact pass polarizers [13], [14], heat-assisted magnetic recording [15], biosensors [16], [17] or refractive index sensing sensors [18]. Plasmonic waveguides have an excellent capability of mode confinement at a deep-subwavelength size, which were introduced to overcome the limits caused by the optical diffraction effect using the conventional dielectric waveguides. This intriguing property is achieved by SPPs created by the coupling between light and collective oscillations of free electrons at the metallic surface. The mode confinement fundamentally depends on the geometrical structure of the plasmonic waveguide and metal used for forming the metal/dielectric interface. To date, various types of plasmonic waveguides have been proposed for improving the propagation length while keeping the propagation mode area at a sub-wavelength size such as metallic nanowires [19], metal strips [20], and wedge-shaped waveguides
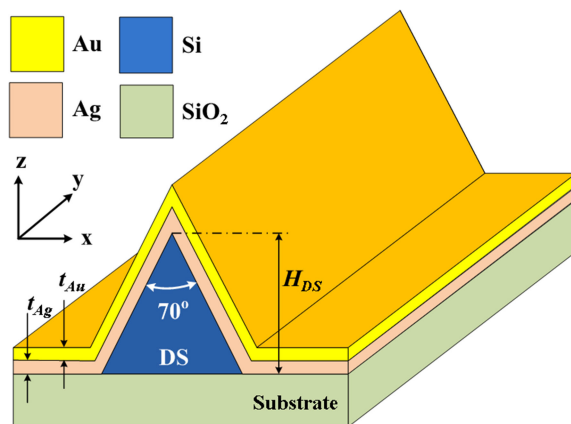
Fig. 1. Schematic of metallic double-layer wedge plasmonic waveguide. The dielectric support is first covered by a thin Ag layer which has a good lightwave guiding property but is sensitive to the operating medium. The thin second layer, Au, is inert to operation medium for protecting. The dimensional parameters of the device are denoted in the figure. The apex angle of the dielectric support is fixed at 70°.

[7]–[10], [21]–[23]. Among these waveguides, wedge-shaped plasmonic waveguides are considered to be an important approach to light confinement due to their excellent capability of the tight light confinement around the apex of the metallic wedge [10]. Furthermore, several types of metals for guiding SPP waves have also been investigated [24], [25]. Among them, Ag metal shows to be superior in the ability of the surface wave guiding than other metals [25], [26]; however, it is sensitive to the operating medium and is easily oxidized. This issue leads to degrade the performance of plasmonic waveguides.

In this study, we propose a metallic double-layer structure to overcome the above-mentioned problems and to enhance the propagation length of SPPs. The structure consists of a Si wedge covered first by an Ag layer and then by an outer thin protective Au layer. We investigate the propagation properties of the SPP wave using this structure at various layer parameters. To evaluate the performance of the proposed waveguide structure, we compare its propagation characteristics with an identical waveguide structure using a single Au wedge. Finally, we further apply the new metallic double-layer structure to the performance of wedge-to-wedge hybrid plasmonic waveguides.

2. Model of Plasmonic Waveguide Using Wedge-Shaped Metallic Double-Layer Structure

The structure of the proposed plasmonic waveguide is shown in Fig. 1. The device consists of a metallic double-layer structure, in which a thin Au layer which is stable to the operating medium is deposited on an Ag layer unstable to operating medium such as air or aqueous environments. In these operating environments, silver thin films are tarnished, so various solutions have been proposed to protect the silver thin films such as coating dielectric multilayers (Ta_2O_5/SiO_2 multilayers) [27], a functionalized layer [28], or silver–gold alloy films [29]. The Ag film has better SPP wave guiding ability than the Au film. The wedge-shaped metal two-layer plasmonic waveguide can be fabricated by depositing the metal layers sequentially on a wedge-shaped dielectric support (DS) [29]–[31]. To deposit metal thin layers on top of the wedge-shaped dielectric support, especially to a sharp wedge, is a challenge to recent technology. However, using layer-by-layer and epitaxial growth methods, thin Au and Ag layers can be formed [30], [31], in which the roughness of deposited Au and Ag films is less than 0.36 nm. Moreover, in ref. [29], simultaneously depositing Au and Ag films using the thermal evaporation technique forms an ultra-thin silver—gold alloy film that can protect the Ag film from oxidization. In our simulation study, we assumed that the surface of metal
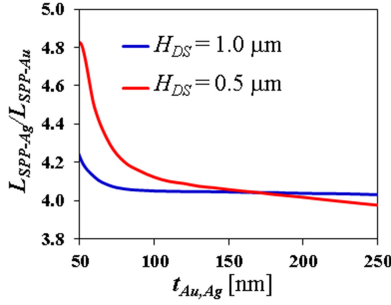
Fig. 2. Thickness dependence of the propagation length ratio for wedge plasmonic waveguides with a single layer of Au or Ag for two different heights of the dielectric support, $H_{DS} = 0.5\,\mu$m and 1 μm. Here t_{Au} and t_{Ag} are the thicknesses of Au and Ag, respectively.

films are perfectly flat and continuous, however, the imperfect of the deposited metal films such as the grain boundary and surface roughness can increase the SPP propagation loss.

To evaluate the working performance of the proposed device, we compare the propagation characteristics with that of the conventional metal wedge plasmonic waveguide (Single metal wedge plasmonic waveguide). We will characterize the propagation length of these devices depending on the thicknesses of the Au (t_{Au}) and the Ag (t_{Ag}) metallic layers at the optical telecommunication wavelength of 1.55 μm. At this wavelength, the complex refractive indexes of Ag and Au are 0.15649–11.567i and 0.23823–11.263i, respectively. For simple, we choose single crystal silicon for DS with the refractive index of 3.4757 and silicon dioxide for the substrate with the refractive index of 1.4957. Silicon is chosen to build the device due to the fact that in comparison with other platforms, the size of plasmonic waveguides based on silicon platform can be reduced owing to the high refractive index of silicon [32]. The similar advantage can also be found in InP platform [33]. In this paper, the apex angle of DS is 70° for all investigations. In general, this typical DS can be fabricated using wet anisotropic etching of single crystal silicon in potassium solution [34]. To obtain a comprehensive view of the current study, we first consider the propagation characteristics of plasmonic waveguides made of single Ag and Au wedges. The whole waveguide is embedded in air with the refractive index of 1.0. The propagation length ratio between the Ag and Au wedge plasmonic waveguides, L_{SPP-Ag}/L_{SPP-Au}, for two different heights of DS, $H_{DS} = 0.5\,\mu$m and 1 μm, as a function of the thickness of the metal layers, t_{Au} and t_{Ag}, are shown in Fig. 2. In which the propagation length is calculated by [35]

$$L_{SPP} = 1/\left(2\left[\mathrm{Im}\left(\beta\right)\right]\right), \tag{1}$$

where β is the wave propagation constant along the waveguide, y-axis (Fig. 1). This constant was obtained from solving the Helmholtz equation using the boundary mode analysis problem in the finite element method based COMSOL Multiphysics [35]. It is shown that, in the investigated range of t_{Au} and t_{Ag}, from 50 nm to 250 nm, L_{SPP-Ag}/L_{SPP-Au} is always larger than 4, Fig. 2. Furthermore, the effective mode area of the Ag wedge plasmonic waveguide is $\lambda^2/(1.3 \times 10^5)$ which is the same as that of the Au wedge plasmonic waveguide. Here, the effective mode area, A_{eff}, is calculated via expression [35],

$$A_{eff} = \int\int_{-\infty}^{\infty} \frac{W(x,z)dxdz}{\max W(x,z)}, \tag{2}$$

where, $W(x,z)$ is the electromagnetic energy density defined as:

$$W(x,z) = \frac{1}{2}\mathrm{Re}\left\{\frac{d\left[\omega\varepsilon(x,z)\right]}{d\omega}\right\}\left|E(x,z)\right|^2 + \frac{1}{2}\mu_0\left|H(x,z)\right|^2, \tag{3}$$

where, $E(x,z)$ and $H(x,z)$ are the electric and magnetic fields, $\varepsilon(x,z)$ is the electric permittivity and μ_0 is the vacuum magnetic permeability. Thus, the SPP wave guiding ability of wedge plasmonic
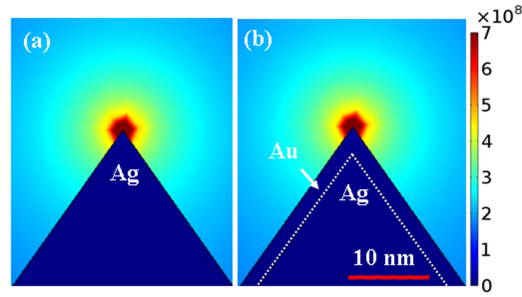
Fig. 3. Normalized electric field distributions of wedge SPP mode of the Ag wedge plasmonic waveguide (a) and the Au/Ag two-layer wedge plasmonic waveguide (b), embedded in air. The height of the dielectric supports for both cases is 1 μm.
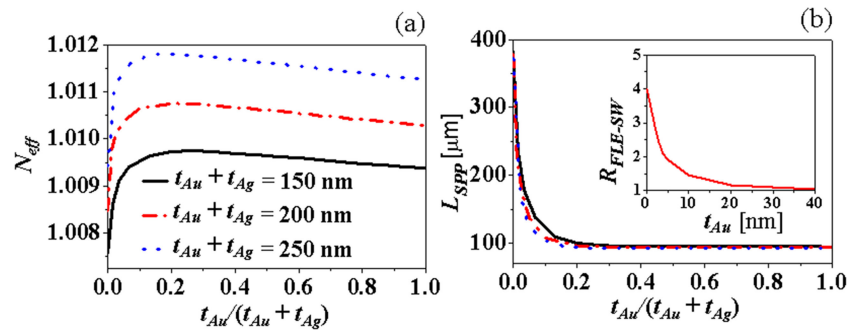

Fig. 4. Effective mode index (N_{eff}) (a) and propagation length ($L_{SPP-Au/Ag}$) (b) of the plasmonic waveguide using the Au/Ag two-layer wedge structure depending on $t_{Au}/(t_{Au} + t_{Ag})$. The inset in (b) is the propagation length enhancing factor, R_{FLE-SW}, as a function of t_{Au} for case $t_{Au} + t_{Ag} = 250$ nm.

waveguide made of Ag is superior to that made of Au. Now, we turn to comparatively investigate the propagation characteristics of the proposed plasmonic waveguide and the conventional metal wedge waveguide as a function of the thickness ratio between the Au layer (t_{Au}) and the Ag (t_{Ag}) layer. The normalized electric field distributions of wedge SPP mode of the Ag wedge plasmonic waveguide and the proposed plasmonic waveguide embedded in air are shown in Fig. 3. The electric field distributions of the two waveguides are almost the same.

We now turn to investigate the modal characteristics of the plasmonic waveguide using the Au/Ag two-layer structure, the mode index (N_{eff}) and the propagation length ($L_{SPP-Au/Ag}$), depending on the thickness ratio between the Au layer and the total two-layer, $t_{Au}/(t_{Au} + t_{Ag})$. The investigated results of N_{eff} and $L_{SPP-Au/Ag}$ depending on $t_{Au}/(t_{Au} + t_{Ag})$ for three different total thicknesses, $t_{Au} + t_{Ag} = 150$ nm, 200 nm, and 250 nm, are shown in Fig. 4. The total thickness is chosen in the range of 150–250 nm, because it is suitable for practice applications. Moreover, at a metal thickness larger than 150 nm, the mode coupling effect between the SPP modes at the metal/DS interface and the wedge SPP mode is eliminated. Fig. 4 shows N_{eff} and $L_{SPP-Au/Ag}$ strongly varying in the range of $0 \leq t_{Au}/(t_{Au} + t_{Ag}) \leq 0.16$. When $t_{Au}/(t_{Au} + t_{Ag}) > 0.16$, N_{eff} and $L_{SPP-Au/Ag}$ are almost unchanged with $t_{Au}/(t_{Au} + t_{Ag})$. When $t_{Au}/(t_{Au} + t_{Ag}) = 0$, the Au/Ag two-layer wedge structure becomes the single Ag layer wedge structure and when $t_{Au}/(t_{Au} + t_{Ag}) = 1$, the Au/Ag two-layer wedge structure becomes the single Au layer wedge structure. From Fig. 4 (b), it shows that $L_{SPP-Au/Ag}$ decreases quickly with $t_{Au}/(t_{Au} + t_{Ag})$, i.e., when the thickness of the Ag layer decreases. This observation is in good agreement with the results from Fig. 2 because the propagation length of the Ag wedge plasmonic waveguide is about 4 times higher than that of the Au one. In general, with ($t_{Au} + t_{Ag}$) in the range of 150–250 nm, the curves of $L_{SPP-Au/Ag}$ are almost overlapping, Fig. 4 (b). We define the propagation length enhancing factor, (R_{FLE-SW}), to be the ratio
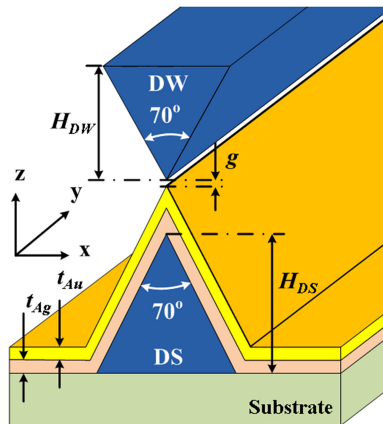
Fig. 5. Schematic of hybrid plasmonic waveguide employed the Au/Ag double-layer wedge structure. The parameters of the metal wedge are the same as of Fig. 1. H_{DW} is the height of the dielectric waveguide and g is the gap between the dielectric waveguide and the metal wedge. The apex angle of the dielectric waveguide as well as the metal wedge is 70°.

of propagation length between the Au/Ag and Au wedge plasmonic waveguides, $R_{FLE-SW} = L_{SPP-Au/Ag}/L_{SPP-Au}$. The explicit dependence of R_{FLE-SW} on t_{Au} is shown in the inset of Fig. 4(b). Clearly, when $t_{Au} \leq 40\,\text{nm}$, R_{FLE-SW} is larger than 1, i.e., the propagation length of the Au/Ag wedge plasmonic waveguide is enhanced compared to that of the Au wedge plasmonic waveguide. When $t_{Au} = 2\,\text{nm}$, $t_{Au} + t_{Ag} = 200\,\text{nm}$ and $H_{DW} = 0.5\,\mu\text{m}$, the propagation length of the wedge plasmonic waveguide with the Au/Ag two-layer structure is 231 μm, which decreases 39%, compared with that of the Ag wedge plasmonic waveguide without depositing Au (378 μm); however, its propagation length is still larger than 2.47 times compared to that of the Au wedge plasmonic waveguide (93 μm).

In the investigated range, the effective mode area, A_{eff}, which is defined as $\lambda^2/(1.31 \times 10^5)$, is almost unchanged. Moreover, the figure of merit, $FoM = L_{SPP-Au/Ag}/\text{sqrt}(A_{eff})$ [36], also decreases 2.5 times, from 4.78×10^4 (Au/Ag wedge plasmonic waveguide) to 1.94×10^4 (Au wedge plasmonic waveguide).

3. Metal Two-Layer Interface in Hybrid Plasmonic Waveguides

The above investigations show that we can increase the propagation length of Au metal wedge plasmonic waveguides by a factor of 2.5 by using the Au/Ag two-layer wedge structure. Such wedge plasmonic waveguides have been interested in applications such as guiding waves at the nanoscale, sensing applications, and nanolasers [1], [6]–[17]. However, the high propagation attenuation causing by ohmic loss limits the applications of the single wedge plasmonic waveguides. The recent developments show that the hybrid wedge plasmonic waveguides exhibit excellent capacity in the low loss light wave propagation at deep-subwavelength size [21], [22]. Therefore, we will here further apply the new wedge-shaped Au/Ag double-layer structure on the modal characteristics of the hybrid wedge plasmonic waveguide. The structure of the device is shown in Fig. 5. The physical parameters of the metal wedge are the same as those shown in Fig. 1 with some additional parameters presented in Fig. 5.

We study the hybrid gap plasmon mode in the device which is created by the hybridization between the wedge SPP mode and the dielectric waveguide (DW) photonic mode [35]. Normalized electric field distributions and field profile along the A-A' cut line (Fig. 6 (a)) of hybrid gap plasmon mode of the hybrid plasmonic waveguide for two different heights of DW, $H_{DW} = 0.5\,\mu\text{m}$ and $H_{DW} = 1.0\,\mu\text{m}$, are shown in Figs. 6(a–b) and Figs. 6(c–d), respectively. It is clear from Fig. 6 that the field energy concentration in the hybrid gap plasmon mode and the DW photonic mode depends on H_{DW}.
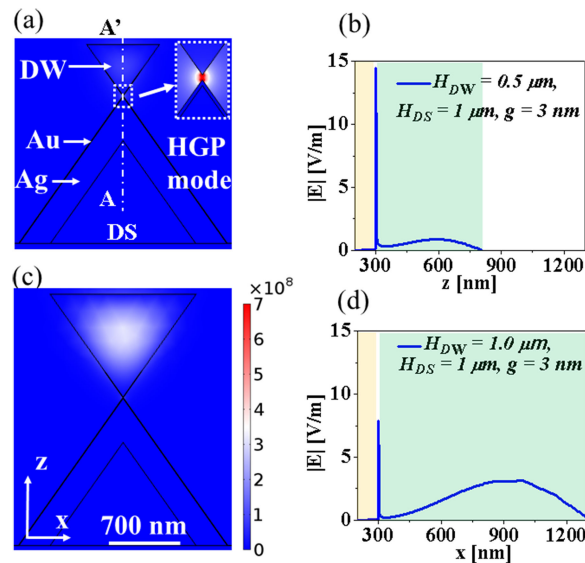
Fig. 6. Normalized electric field distributions of hybrid plasmonic waveguides. (a) and (b) are the field profile in two-dimensional and along the A-A' cut line (in (a)) for $H_{DW} = 0.5\,\mu$m, respectively. (c) and (d) for the height of $H_{DW} = 1\,\mu$m. In (b) and (d), the dielectric regions are no shading regions; the shaded pink and green areas represent the metal and DW regions, respectively. In these investigations, the height of DS H_{DS} is 1.0 μm and the dielectric gap g is 3 nm. The inset in (a) shows a magnification of the hybrid gap plasmon mode.

At $H_{DW} = 0.5\,\mu$m, the field energy of the device almost concentrates into the hybrid gap plasmon mode, Figs. 6 (a) and (b). When varying g, we can also control the field energy distribution in either the hybrid gap plasmon mode or the DW photonic mode [35]. However, the mode energy distribution is independent of H_{DS}. This observation can be explained from the fact that the hybrid gap plasmonic mode is created by the hybridization between the wedge SPP mode and the DW photonic mode. The dependence of mode energy distribution on H_{DS} differs with the single metal wedge waveguide in which the propagation characteristics depends on H_{DS} [10]. In the above investigations, we used the dielectric gap, $g = 3$ nm, that is feasible for fabrication with the recent advancements of thin film depositing technologies [30], [31], [35], [37].

Having studied the electric field distribution in the hybrid plasmonic waveguide, we will now focus on the effect of enhancing the propagation length of the device using the Au/Ag double-layer structure. We use the device with the dimensional parameters the same as in Fig. 6 (a), except the thickness of the two metal layers. Figure 7 shows the dependence of the modal characteristics of the hybrid plasmonic waveguide including the effective refractive index N_{eff}, the propagation length $L_{HGP-Au/Ag}$, the normalized mode area A_{eff}/A_o, and the figure of merit FoM, on the thickness ratio between the Au layer and the total Au + Ag layers, $t_{Au}/(t_{Au} + t_{Ag})$. There is no significant difference of N_{eff} and $L_{HGP-Au/Ag}$ behaviors between the hybrid plasmonic waveguide and the Au/Ag double-layer wedge plasmonic waveguide, Fig. 4. $L_{HGP-Au/Ag}$ decreases quickly with $t_{Au}/(t_{Au} + t_{Ag})$. Similar to the Au/Ag wedge plasmonic waveguide investigated above, we also define the factor of propagation length enhancement of the hybrid plasmonic waveguide, $R_{FLE-HW} = L_{HGP-Au/Ag}/L_{HGP-Au}$. R_{FLE-HW}, the inset in Fig. 7 (b). This factor is always larger than 1 when $t_{Au} \leq 40$ nm similar to that of the Au/Ag wedge plasmonic waveguide. Fig. 7 (b) shows that the propagation length, $L_{HGP-Au/Ag}$ is almost independent to $t_{Au}/(t_{Au} + t_{Ag})$ at this ratio >0.16. When $t_{Au}/(t_{Au} + t_{Ag}) = 0.01$, i.e., $t_{Au} = 2$ nm and $t_{Ag} = 248$ nm, $L_{HGP-Au/Ag}$ of the hybrid plasmonic waveguide using the Au/Ag double-layer wedge structure ($\sim$2.55 mm) is 2.5 times larger than that of using the Au wedge structure ($\sim$1.01 mm) with the identical waveguide structure. Furthermore, in the investigated range, the effective mode area is independent to $t_{Au}/(t_{Au} + t_{Ag})$. Therefore, the curve of FoM has a similar
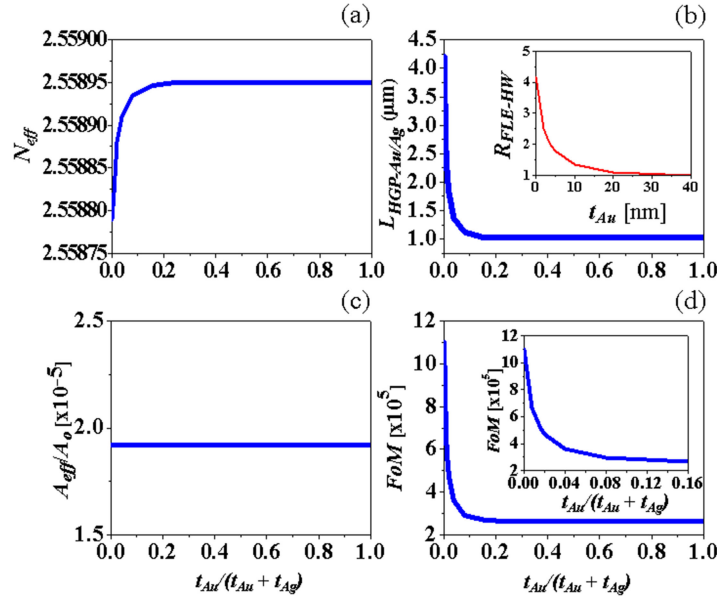
Fig. 7. Dependence of the modal characteristics of the hybrid plasmonic waveguide on the thickness ratio between the Au layer and the total metal layers, $t_{Au}/(t_{Au} + t_{Ag})$. They are (a) the effective refractive index N_{eff}, (b) the propagation length $L_{HGP-Au/Ag}$, (c) the normalized mode area A_{eff}/A_o, and (d) the figure of merit *FoM*. The dimensional parameters of the hybrid plasmonic waveguide are fixed as in Fig. 6 (a), except the thickness of the two metal layers. The inset in (b) shows R_{FLE-HW} as a function of t_{Au} for case $t_{Au} + t_{Ag} = 250$ nm. The inset in (d) shows the curve of *FoM* with $t_{Au}/(t_{Au} + t_{Ag})$ from 0–0.16.
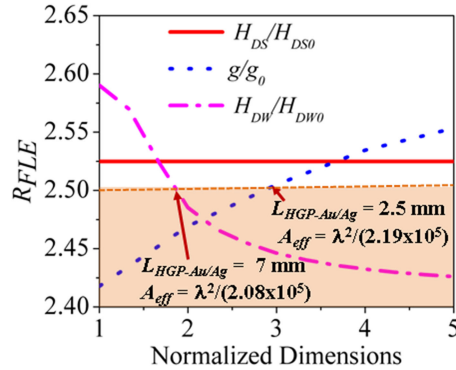

Fig. 8. Dependence of the ratio of propagation length between the Au/Ag and Au wedge hybrid plasmonic waveguides on the normalized dimensions, H_{DS}/H_{DS0} (g = 3 nm, $H_{DW} = 1\,\mu$m, and $H_{DS0} = 0.3\,\mu$m), g/g_0 ($g_0 = 1$ nm, $H_{DW} = 0.5\,\mu$m, and $H_{DS} = 1\,\mu$m), and H_{DS}/H_{DS0} (g = 3 nm, $H_{DS0} = 0.3\,\mu$m, and $H_{SD} = 1\,\mu$m). The metal two-layer interface consists of 2 nm Au and 248 nm Ag.

shape to that of $L_{HGP-Au/Ag}$ (Fig. 7 (b)). The inset in Fig. 7 (d) shows a strong dependence of *FoM* on $t_{Au}/(t_{Au} + t_{Ag})$ in the range of 0–0.16.

    To obtain a comprehensive understanding the enhancement of the propagation length of the hybrid plasmonic waveguide using the metallic double-layer structure, we investigate the enhancement factor, R_{FLE-HW}, as a function of normalized dimensions, the height of DS (H_{DS}/H_{DS0}), the dielectric gap g/g_0, and the height of DW (H_{DW}/H_{DW0}). The results are shown in Fig. 8. As can be seen, R_{FLE-HW} is almost independent to H_{DS} while it shows increasing and decreasing relations on g and H_{DW}, respectively. In the investigated range of H_{DS}, g, and H_{DW}, R_{FLE-HW} is always larger than 2.42. Under the conditions, $H_{DW}/H_{DW0} \leq 2$ and $g/g_0 \geq 3$ (no shading region in Fig. 8),

we can increase the propagation length of the hybrid wedge-shaped plasmonic waveguide by at least 2.5 times using the Au/Ag double-layer wedge structure instead of the single Au wedge structure. The proposed hybrid plasmonic waveguide can obtain a long-distance lightwave propagation ($\geq$7 mm) with deep-subwavelength size ($\leq\lambda^2/(2.08 \times 10^5)$). It is important to notethat A_{eff} is independent to H_{DW} while $L_{HGP-Au/Ag}$ decreases with H_{DW}. Furthermore, $L_{HGP-Au/Ag}$ and A_{eff} are proportional to g. Therefore, we can compromisely control H_{DW} and g to obtain the propagation length enhancing factor which is higher than 2.5 while the hybrid plasmonic waveguide still obtains a long propagation length at the deep-subwavelength size.

4. Conclusions

We have proposed a metallic double-layer structure for improving the propagation length of surface plasmon polaritons. The structure consists of a metal which has a good plasmon wave guiding property but is unstable to the operating medium covered by a protective stable metallic layer. Using the Ag wedge covered by a thin Au layer, the propagation length of surface plasmon polaritons can be enhanced by a factor of 2.5 compared to that using the single Au wedge. The advantage of the proposed metallic double-layer structure is also preserved in the hybrid plasmonic waveguides in which we can obtain a long-distance lightwave propagation ($\geq$7 mm) at the deep-subwavelength size ($\leq\lambda^2/(2.08 \times 10^5)$).

References

[1] Y. Bian *et al.*, "Modal properties of triangular metal groove/wedge based hybrid plasmonic structures for laser actions at deep-subwavelength scale," *Opt. Commun.*, vol. 297, pp. 102–108, 2013.

[2] A. Tasolamprou, D. Zografopoulos, and E. Kriezis, "Liquid crystal-based dielectric loaded surface plasmon polariton optical switches," *J. Appl. Phys.*, vol. 110, no. 9, 2011, Art. no. 093102.

[3] J. S. Smalley *et al.*, "High contrast modulation of plasmonic signals using nanoscale dual-frequency liquid crystals," *Opt. Exp.*, vol. 19, no. 16, pp. 15265–15274, 2011.

[4] A. A. R. Mohamed, L. A. Shahada, and M. A. Swillam, "Electro-optic plasmonic modulator with direct coupling to silicon waveguides," *IEEE Photon. J.*, vol. 9, no. 6, Dec. 2017, Art. no. 4502807.

[5] M. I. Stockman *et al.*, "Roadmap on plasmonics," *J. Opt.*, vol. 20, no. 4, 2018, Art. no. 043001.

[6] Y. Fang and M. Sun, "Nanoplasmonic waveguides: Towards applications in integrated nanophotonic circuits," *Light Sci. Appl.*, vol. 4, no. 6, 2015, Art. no. e294.

[7] R. Hao, E. Cassan, Y. Xu, Q. Min, X. Wei, and E. P. Li, "Reconfigurable parallel plasmonic transmission lines with nanometer light localization and long propagation distance," *IEEE J. Sel. Topics Quantum Electron.*, vol. 19, no. 3, May/Jun. 2013, Art. no. 4601809.

[8] D. Martín-Cano, L. Martín-Moreno, F. J. Garci´a-Vidal, and E. Moreno, "Resonance energy transfer and superradiance mediated by plasmonic nanowaveguides," *Nano Lett.*, vol. 10, pp. 3129–3134, 2010.

[9] S. J. Kress *et al.*, "Wedge waveguides and resonators for quantum plasmonics," *Nano Lett.*, vol. 15, pp. 6267–6275, 2015.

[10] E. Moreno, S. G. Rodrigo, S. I. Bozhevolnyi, L. Martín-Moreno, and F. García-Vidal, "Guiding and focusing of electromagnetic fields with wedge plasmon polaritons," *Phys. Rev. Lett.*, vol. 100, 2008, Art. no. 023901.

[11] N. Abadýa *et al.*, "Low-power consumption Franz-Keldysh effect plasmonic modulator," *Opt. Exp.*, vol. 22, no. 9, 2014, Art. no. 11236.

[12] N. Abadia, S. Olivier, D. Marris-Morini, L. Vivien, T. Bernadin, and J. C. Weeber, "A CMOS-compatible Franz-Keldysh effect plasmonic modulator," in *Proc. 11th Int. Conf. Group IV Photon.*, 2014, pp. 63–64.

[13] N. Abadýa *et al.*, "CMOS-compatible multi-band plasmonic TE-pass polarizer," *Opt. Exp.*, vol. 26, no. 23, pp. 30292–30304, 2018.

[14] Z. Ying, G. Wang, X. Zhang, Y. Huang, H.-P. Ho, and Y. Zhang, "Ultracompact TE-pass polarizer based on a hybrid plasmonic waveguide," *IEEE Photon. Technol. Lett.*, vol. 27, no. 2, pp. 201–204, Jan. 2015.

[15] N. Abadýa *et al.*, "Optical and thermal analysis of the light-heat conversion process employing an antenna-based hybrid plasmonic waveguide for HAMR," *Opt. Exp.*, vol. 26, no. 4, 2018, Art. no. 1752.

[16] P. Debackere, S. Scheerlinck, P. Bienstman, and R. Baets, "Surface plasmon interferometer in silicon-on-insulator: Novel concept for an integrated biosensor," *Opt. Exp.*, vol. 14, pp. 7063–7072, 2006.

[17] H. K. Mulder, A. Ymeti, V. Subramaniam, and J. S. Kanger, "Size-selective detection in integrated optical interferometric biosensors," *Opt. Exp.*, vol. 20, pp. 20934–20950, 2012.

[18] A. Paliwal, M. Tomar, and V. Gupta, "Refractive index sensor using long-range surface plasmon resonance with prism coupler," *Plasmonics*, vol. 14, no. 2, pp. 375–381, 2019.

[19] S. Ghosh and B. Rahman, "Evolution of plasmonic modes in a metal nano-wire studied by a modified finite element method," *J. Lightw. Technol.*, vol. 36, no. 3, pp. 809–818, Feb. 2018.

[20] B. Sturlesi, M. Grajower, N. Mazurski, and U. Levy, "Integrated amorphous silicon-aluminum long-range surface plasmon polariton (LR-SPP) waveguides," *APL Photon.*, vol. 3, 2018, Art. no. 036103.

[21] Y. Ma, G. Farrell, Y. Semenova, and Q. Wu, "A hybrid wedge-to-wedge plasmonic waveguide with low loss propagation and ultra-deep-nanoscale mode confinement," *J. Lightw. Technol.*, vol. 33, no. 18, pp. 3827–3835, Sep. 2015.

[22] Y. Bian and Q. Gong, "Deep-subwavelength light confinement and transport in hybrid dielectric-loaded metal wedges," *Laser Photon. Rev.*, vol. 8, pp. 549–561, 2014.

[23] L. Ding, J. Qin, K. Xu, and L. Wang, "Long range hybrid tube-wedge plasmonic waveguide with extreme light confinement and good fabrication error tolerance," *Opt. Exp.*, vol. 24, no. 4, pp. 3432–3440, 2016.

[24] M. P. Nielsena, A. Ashfar, K. Cadien, and A. Y. Elezzabi, "Plasmonic materials for metal–insulator–semiconductor–insulator–metal nanoplasmonic waveguides on silicon-on-insulator platform," *Opt. Mater.*, vol. 36, no. 2, pp. 294–298, 2013.

[25] S. A. Maier, *Plasmonics: Fundamentals and Applications.* Berlin, Germany: Springer, 2007.

[26] "Optical properties of the metals Al, Co, Cu, Au, Fe, Pb, Ni, Pd, Pt, Ag, Ti, and W in the infrared and far infrared," *Appl. Opt.*, vol. 22, no. 7, pp. 1099–1120, 1983.

[27] G. Manickam *et al.*, "Protection and functionalisation of silver as an optical sensing platform for highly sensitive SPR based analysis," *Analyst*, vol. 137, pp. 5265–5271, 2012.

[28] D. Y. Song, R. W. Sprague, H. A. Macleod, and M. R. Jacobson, "Progress in the development of a durable silver-based high-reflectance coating for astronomical telescopes," *Appl. Opt.*, vol. 24, no. 8, pp. 1164–1170, 1985.

[29] M. Zhou, Y. Cai, Y. P. Li, and D. Q. Liu, "Durability of ultra-thin silver films and silver—Gold alloy films under UV irradiation," *Chinese Phys. Lett.*, vol. 33, no. 10, 2016, Art. no. 107803.

[30] L. Leandro, R. Malureanu, N. Rozlosnik, and A. Lavrinenko, "Ultrathin, ultrasmooth gold layer on dielectrics without the use of additional metallic adhesion layers," *ACS Appl. Mater. Interfaces*, vol. 7, pp. 5797–5802, 2015.

[31] Y. Wu *et al.*, "Intrinsic optical properties and enhanced plasmonic response of epitaxial silver," *Adv. Mater.*, vol. 26, pp. 6106–6110, 2014.

[32] M. Barturen, N. Abadía, J. Milano, P. A. Costanzo Caso, and D. V. Plant, "Manipulation of extinction features in frequency combs through the usage of grapheme," *Opt. Exp.*, vol. 26, no. 12, 2018, Art. no. 15490.

[33] N. Abadía *et al.*, "Highly fabrication tolerant InP based polarization beam splitter based on p-i-n structure," *Opt. Exp.*, vol. 25, no. 9, 2017, Art. no. 10070.

[34] B. Ku, K. S. Kim, Y. Kim, and M. S. Kwon, "Bulk-silicon-based waveguides and bends fabricated using silicon wet etching: Properties and limits," *J. Lightw. Technol.*, vol. 35, no. 18, pp. 3918–3923, Sep. 2017.

[35] R. F. Oulton, V. J. Sorger, D. Genov, D. Pile, and X. Zhang, "A hybrid plasmonic waveguide for subwavelength confinement and long-range propagation," *Nature Photon.*, vol. 2, pp. 496–500, 2008.

[36] R. Buckley and P. Berini, "Figures of merit for 2D surface plasmon waveguides and application to metal stripes," *Opt. Exp.*, vol. 15, pp. 12174–12182, 2007.

[37] R. F. Oulton *et al.*, "Plasmon lasers at deep subwavelength scale," *Nature*, vol. 461, pp. 629–632, 2009.